DE GRUYTER OPEN

Acta Geophysica
vol. 63, no. 4, Aug. 2015, pp. 978-999
DOI: 10.1515/acgeo-2015-0017

Permeability Evolution and Rock Brittle Failure

Qiang SUN[1], Lei XUE[2], and Shuyun ZHU[1]

[1]School of Resources and Geosciences, China University of Mining and Technology, Xuzhou, China; e-mail: sunqiang04@126.com

[2]Key Laboratory of Shale Gas and Geoengineering, Institute of Geology and Geophysics, Chinese Academy of Sciences, Beijing, China

Abstract

This paper reports an experimental study of the evolution of permeability during rock brittle failure and a theoretical analysis of rock critical stress level. It is assumed that the rock is a strain-softening medium whose strength can be described by Weibull's distribution. Based on the two-dimensional renormalization group theory, it is found that the stress level λ_c (the ratio of the stress at the critical point to the peak stress) depends mainly on the homogeneity index or shape parameter m in the Weibull's distribution for the rock. Experimental results show that the evolution of permeability is closely related to rock deformation stages: the permeability has a rapid increase with the growth of cracks and their surface areas (*i.e.*, onset of fracture coalescence point), and reaches the maximum at rock failure. Both the experimental and analytical results show that this point of rapid increase in permeability on the permeability-pressure curve corresponds to the critical point on the stress-strain curve; for rock compression, the stress at this point is approximately 80% of the peak strength. Thus, monitoring the evolution of permeability may provide a new means of identifying the critical point of rock brittle fracture.

Key words: microfracturing, critical information, permeability evolution.

1. INTRODUCTION

Rock permeability is strongly influenced by the deformation of the rock and controlled by the evolution of the geometrical structure of cracks and pore space (volume, connectivity, tortuosity, shape, *etc.*). Depending on the initial porosity and the stress acting on the rock, compaction and strain hardening or, on the contrary, dilation and strain softening may occur (Sulem and Ouffroukh 2006).

A better understanding of the evolution of permeability was initiated through the experimental work of Brace *et al*. (1968), who first applied the pulse decay method in triaxial tests of granites to measure their permeability under high pressure. In the past half century, significant achievements have been made in systematic studies on the evolution of permeability during rock cracking. The permeability may decrease slightly under the application of relatively small stresses, but when the stress is further increased, a threshold level is usually found, above which the permeability increases very markedly, even under confining pressure (*e.g.*, Brace *et al*. 1968, Mordecai and Morris 1971, Zoback and Byerlee 1975a, b; Walsh and Brace 1984, Wong *et al.* 1997, Zhu and Wong 1996, 1997, 1999, Yang *et al*. 2008, David *et al.* 2001, Lock *et al.* 2002, Paterson and Wong 2005, Liu *et al.* 2009, Zhang *et al*. 2013). This threshold may be closely correlated with the onset of marked Acoustic Emission (AE) (Paterson 1978). Jiang *et al.* (2002) gave the rock permeability-stress mathematical expression before the peak stress is reached, and investigated two characteristic parameters – the critical anti-permeability strength of rock and the initial permeability – according to the rock stress-strain curve and the permeability-strain curve obtained from rocks under complete loading-to-unloading cycles. Wang *et al.* (2006) found that the permeable pressure complies with a negative exponential function of time during rock deformation and failure.

Under an external load, the evolution of rock permeability is influenced by the stress-strain state (Sun *et al.* 2012). In this study, we monitored three parameters: stress, strain, and permeability, for compressed rocks undergone brittle failure, and the evolution of rock permeability is studied experimentally, especially during disintegration and rupture of the rock after the failure stress has been reached.

The renormalization group probability of destruction is also employed to analyze the stress and strain at the critical point of rock brittle failure. The fracturing of stressed materials is analogous to a critical phenomenon at a second-order phase transition or the percolation phenomenon (Martin 1997, Sornette 2000). The moment of rupture is similar to a critical point, so the fracturing process can be described by a renormalization-group scheme (Anifrani *et al.* 1995), and a critical region exists in the vicinity of the critical point of rupture (Sornette and Andersen 1998).

2. PERMEABILITY EVOLUTION AND STRESS-STRAIN OF INTACT ROCKS UNDER COMPRESSION

Several characteristic stresses important for understanding the damage process can be identified from the stress-strain curve shown in Fig. 1. σ_a is the crack closure stress, σ_b is the crack initiation stress, σ_c is the crack damage stress corresponding to long-term rock strength (Martin 1993, 1997), or the critical stress; and σ_d is the peak stress. The crack initiation or threshold stress σ_b is defined as the onset of stable crack growth, which is sometimes defined as the point where the crack volumetric strain deviates from zero. The permeability increases with the growth of cracks. When the damage initiation limit is exceeded, existing cracks start to propagate and new cracks initiate in a stable fashion, but critical rock mass damage is not encountered until the density of crack is sufficient for cracks to coalesce to form shear bands or tensile spalls. This state is defined as the "crack damage stress" (Martin 1997) or "permeability threshold". The crack damage stress σ_c is generally defined as the point when volumetric strain reversal occurs and unstable crack growth begins. It also corresponds to the stress when a drastic increase of permeability is observed. In laboratory tests, σ_c can be considered as the wall strength in massive rocks. Table 1 is the damage stress level (*i.e.*, critical stress level) obtained from triaxial compression tests by permeability-strain and stress-strain curves.

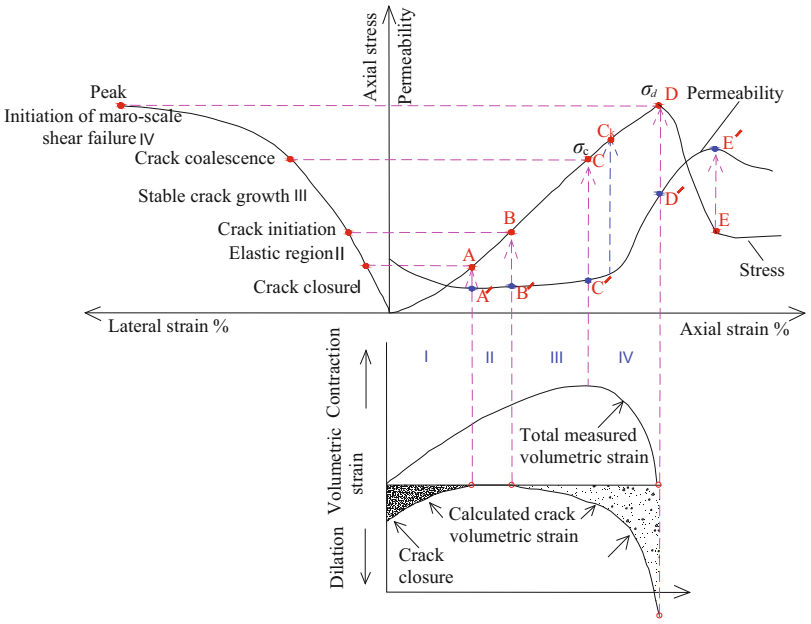

Fig. 1. Corresponding relationship between rock failure and permeability evolution.

Table 1

Relationship between the parameters of rock stress, strain, and permeability

No. of rock samples	Rock type	Confining pressure [MPa]	Pore pressure [MPa]	Differential pressure [MPa]	Point C	
					Strain level [%]	Stress level [%]
1	Coarse sandstone	8	2.8	1.5	82.7	89.1
2	Coarse sandstone	12	2.8	1.5	76.7	83.7
3	Coarse sandstone	16	2.8	1.5	80.8	89.5
4	Coarse sandstone	20	2.8	1.5	62.0	81.2
5	Sandstone	12	2.8	1.5	74.3	83.8
6	Limestone	4	2.8	1.5	65.7	68.7
7	Limestone	4	2.8	1.5	65.3	73.7
8	Medium sandstone	4	2.8	1.5	83.4	75.2
9	Medium sandstone	4	3.8	1.8	80.7	76.4
10	Medium sandstone	4	3.8	1.8	85.2	82.2
11	Fine sandstone	4	3.8	1.8	88.1	82.6
12	Fine sandstone	4	3.8	1.8	73.7	73.5
13	Fine sandstone	20	12.0	1.8	77.4	79.5
Average					76.6	79.9

Changes in permeability were observed as a function of pressure for a variety of crystalline rock samples subjected to confining pressure and pore pressure. For most samples, the permeability dropped slightly when the pressure was less than about 10% of the fracture stress σ_d (stage OA shown in Fig. 1). It started to increase at σ_b and then increased drastically after σ_c was reached, until the maximum permeability was usually reached near to σ_e, which is located at the knee point of the constitutive curve. The stress levels, *i.e.*, σ_c and σ_d, represent important stages in the development of macroscopic failure of intact rocks.

From the laboratory tests, three characteristics of the evolution of permeability were identified (in the following text, strain and stress levels are the normalized strain and stress relative to their peak values, respectively, and permeability level refers to the permeability normalized by its initial value):

- The permeability increases at stress levels by approximately 30-50%.
- The permeability increases drastically near to the critical point C (Fig. 2); however, sometimes the stress level corresponding to this permeability threshold is greater than the stress level at point C (shown as point C_k in Fig. 1), and is as large as approximately 80% of the peak strength. This

result is roughly consistent with the observation of Lockner *et al*. (1992) on the onset of fracture coalescence, which was found to occur at stress levels of approximately 70-80% of the peak strength.

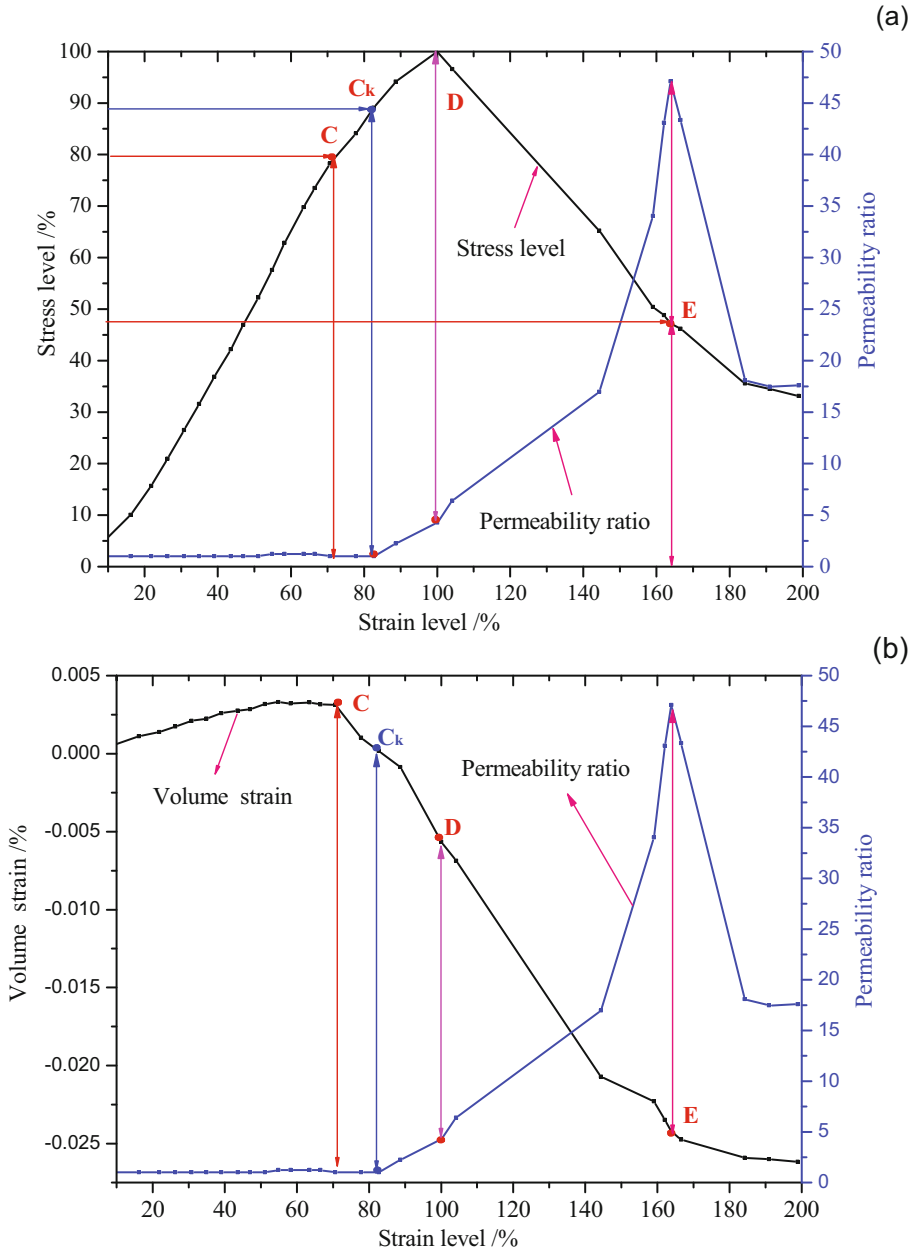

Fig. 2. Continued on next page.

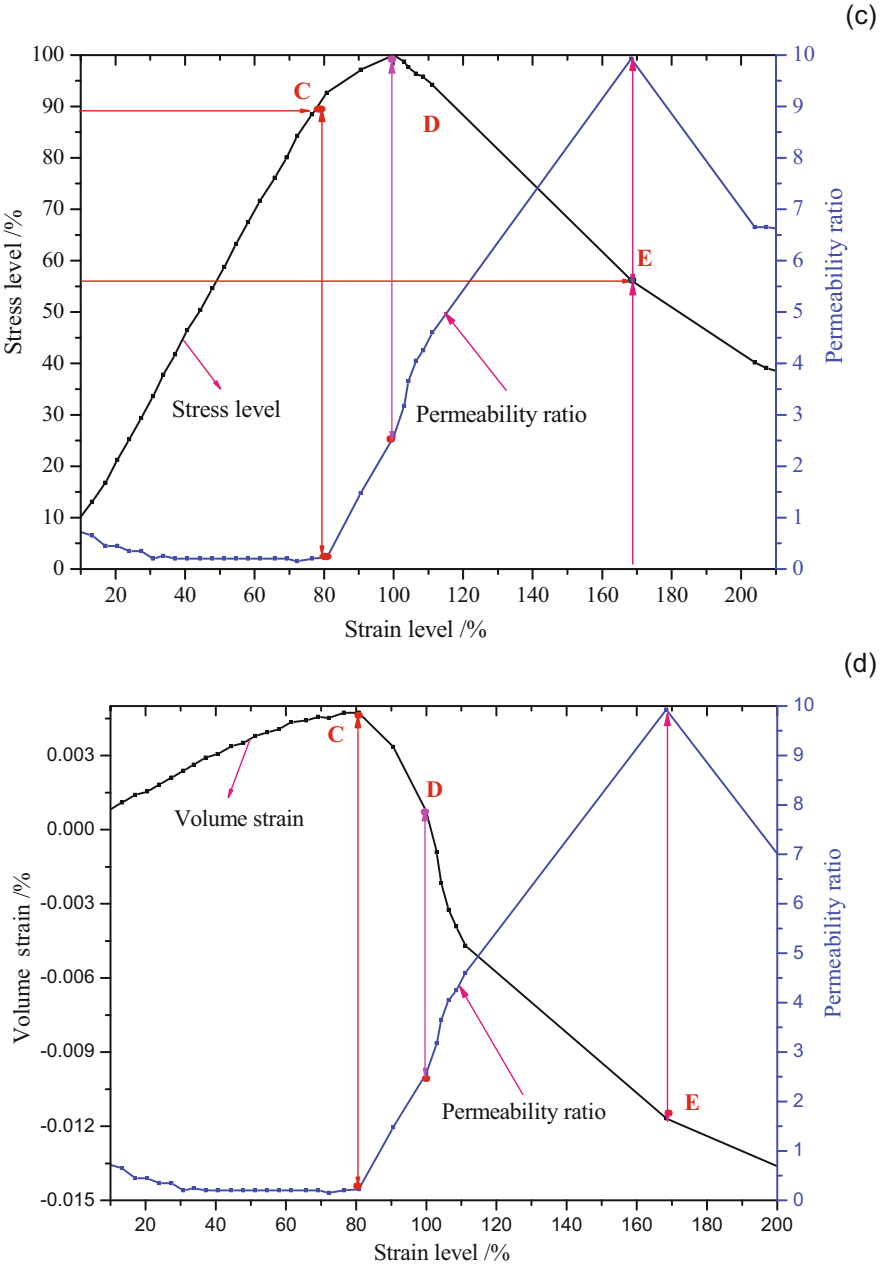

Fig. 2. Relationships between permeability ratio *versus* stress level during loading process for coarse sandstone: (a) coarse sandstone (sample 1 of Table 1), b) coarse sandstone (sample 1 of Table 1), (c) coarse sandstone (sample 3 of Table 1), and (d) coarse sandstone (sample 3 of Table 1).

- Macrocracks or shear-band formation normally occurs at point E, after which the permeability decreases.

3. THEORETICAL ANALYSIS OF STRESS AND STRAIN AT THE CRITICAL POINT

The rock material is considered as a system with a large number of intact rocks resulted from the complexity of formation environment and long-term geological processes. It is well accepted that as the applied load gradually increases, cracks will develop and coalesce around the potential macroscopic fracture plane (Xue 2014). Essentially, only when the crack density of the potential macroscopic fracture plane approaches a certain level, will the macroscopic fracture occur. Therefore, the forming process of the macroscopic fracture plane is simplified and considered as a two-dimensional fracture process in the present work, and two-dimensional renormalization group theory is introduced to describe the failure process of the rock samples (as shown in Fig. 3). Thus, the macroscopic fracture plane can be renormalized into many cells and different order blocks. Here, only the blocks of the first three orders are shown. For example, the first order block comprises four cells, while the second order block consists of four first order blocks. Similarly, the third order block is composed of four second order blocks. In fact, the same combination can be continued to an infinite scale. Furthermore, there exist five possible states for each of the different order blocks, *i.e.*, B4U0, B3U1, B2U2, B1U3, and B0U4 (as shown in Fig. 3d). The uppercase letter "B" denotes that the cells or blocks have broken (colored box), which is followed by the digit corresponding to the number of broken cells or blocks. The uppercase letter "U" means that the cells or blocks have not broken (white box), and the following digit corresponds to the number of unbroken cells or blocks. The corresponding broken probabilities of the five possible states are listed in column B, where p_1 means the broken probability of each cell.

As suggested by Smalley *et al.* (1985), Tang *et al.* (2000), and Wong *et al.* (2006), it is assumed that the strength of each individual cell is σ_{cell}, which obeys a Weibull distribution and depends on the number of micro cracks in the cells. When an external load is applied to a rock sample, it is assumed that each cell of the rock will be subjected to a corresponding local stress. When the strength of the cell σ_{cell} is less than its local stress, the cell will fail and its broken probability is p_α, which can be expressed as:

$$p_\alpha = p\left(\sigma_f < \alpha\sigma\right) = 1 - \exp\left[-\left(\frac{\alpha\sigma}{\sigma_0}\right)^m\right], \tag{1}$$

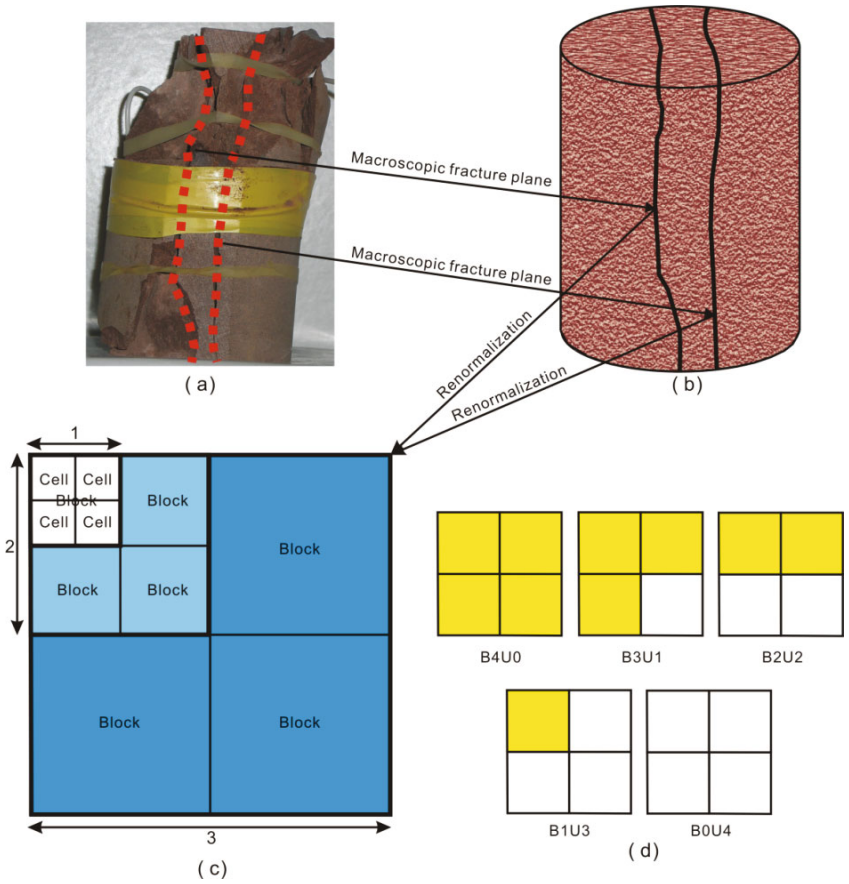

Fig. 3. Illustration of the two-dimensional renormalization group model of macroscopic fracture plane: (a) rock sample with two macroscopic fracture planes after failure under a uniaxial compression test, (b) sketch showing two macroscopic fracture planes, (c) the two-dimensional RG model, and (d) the five possible states for each block (Xue 2014).

where σ is the stress, α is a scale parameter, σ_0 is a measure of average strength, and m is the shape parameter that can be used to evaluate the discreteness of material strength.

The failure probability of elementary blocks corresponding to $\alpha = 1$ can be expressed as

$$p_1 = p\left(\sigma_f < \sigma\right) = 1 - \exp\left[-\left(\frac{\sigma}{\sigma_0}\right)^m\right]. \tag{2}$$

Combining Eqs. 1 with 2, one has

$$p_\alpha = 1-(1-p_1)^{\alpha^m} \ . \tag{3}$$

The conditional probability $p_{\alpha,b}$ for the occurrence of failure (Allegre *et al.* 1982) when a stress $(a-b)\sigma$ is transferred to an unbroken block under stress $b\sigma$ can be written as

$$p_{a,b} = \frac{p\left(b\sigma < \sigma_f < a\sigma\right)}{p\left(\sigma_f > b\sigma\right)} = \frac{P_a - P_b}{1-P_b} \ . \tag{4}$$

According to the renormalization group theory, the probability of destruction at the threshold point of destruction C, p_c, can be derived as

$$p_c = f_c(m) \ . \tag{5}$$

Equation 2 could also be expressed as a probability function of strain, that is,

$$p = 1-\exp\left[-\left(\frac{\varepsilon}{\varepsilon_0}\right)^m\right] , \tag{6}$$

where ε is the axial strain of the rock, and ε_0 is a measurement of average strain.

As the stress-strain constitutive model of rocks can be expressed as (Qin *et al*. 2010a, b)

$$\sigma = E_0 \exp\left[-\left(\frac{\varepsilon}{\varepsilon_0}\right)^m\right] , \tag{7}$$

where E_0 is the initial elastic modulus, the strain value corresponding to the peak strength can be derived by taking the first derivative of Eq. 7 with respect to the stress ε, *i.e.*

$$\varepsilon_d = \left(\frac{1}{m}\right)^{1/m} \varepsilon_0 \ . \tag{8}$$

Inserting Eq. 5 into 6, and then combining with Eq. 8, the strain at the critical failure point C can be derived as

$$\varepsilon_c = \left\{-\ln\left[1-f_c(m)\right]\right\}^{\frac{1}{m}} \varepsilon_0 \ . \tag{9}$$

Divide Eq. 9 by 8, then we have

$$\lambda_c = \frac{\sigma_c}{\sigma_d}\times 100\% = \left\{-m\ln\left[1-f(m)\right]\right\}^{\frac{1}{m}} \exp\left[\frac{1}{m}+\ln\left[1-f(m)\right]\right]\times 100\% \ . \tag{10}$$

Equation 10 gives the relationship between the critical stress level λ_c and the shape parameter.

As one or multiple macroscopic breaking surfaces with sags and crests are usually found on hard and brittle rocks, we assume that the micro-to-macroscopic destruction of rocks samples without joint fissure in the laboratory should be developed in 2D. In order to calculate $f(m)$ in the above equations, the rock material is considered as a system with a large number of intact rocks resulting from the complexity of formation environment and long-term geological processes. The critical behavior of brittle fracture of the rock material will be studied with the model as shown in Fig. 3, which is a 2D lattice renormalization. It is shown in Fig. 3 that a large block is composed of four small blocks, and it has the unique performance. And four large blocks can comprise a larger block, and so forth, that is, according to the process of the renormalization theory. For a group containing two blocks which are either broken or unbroken, the five states are possible: [BBBB], [BBBU], [BBUU], [BUUU], and [UUUU], where the letters "B" and "U" represent a broken block and an unbroken block, respectively. It is easy to conclude that the failure probability $p_1^{(2)}$ of the second-order blocks, which is expressed as Eq. 11, where p_1 is the failure probability of block and $(1-p_1)$ is the unbroken probability.

$$p_1^{(1)} = p_{\mathrm{b}_4\mathrm{u}_0} + p_{\mathrm{b}_3\mathrm{u}_1} + p_{\mathrm{b}_2\mathrm{u}_2} + p_{\mathrm{b}_1\mathrm{u}_3} \ , \tag{11}$$

where

$$p_{\mathrm{b}_4\mathrm{u}_0} = p_1^4 \ , \tag{12}$$

$$p_{\mathrm{b}_3\mathrm{u}_1} = C_4^3 p_1^3 \left(1-p_1\right) p_{4,1} \ , \tag{13}$$

$$p_{\mathrm{b}_2\mathrm{u}_2} = C_4^2 p_1^2 \left(1-p_1\right)^2 \left[p_{2,1}^2 + C_2^1 p_{2,1} \left(1-p_{2,1}\right) p_{4,2} \right] , \tag{14}$$

$$p_{\mathrm{b}_1\mathrm{u}_3} = C_4^1 p_1 \left(1-p_1\right)^3 \begin{bmatrix} p_{4/3,1}^3 + C_3^2 p_{4/3,1}^2 \left(1-p_{4/3,1}\right) p_{4,4/3} \\ +C_3^1 p_{4/3,1} \left(1-p_{4/3,1}\right)^2 \\ \left[p_{2,4/3}^2 + C_2^1 p_{2,4/3} \left(1-p_{2,4/3}\right) p_{4,2} \right] \end{bmatrix} . \tag{15}$$

The threshold probability of destruction under 2D renormalized condition is computed, and the result, $p^* = f(m)$, is also plotted in Fig. 4. It is shown that the peak strength of rock increases with the decrease in shape parameter m, and the calculated 2D mean stress level is 83.2% for m equal to 1, 2, 3, 4, 5, 6, and 7, which is very close to the value of the Darley sandstone tested by Mordecai and Morris (1971), as shown in Fig. 5.

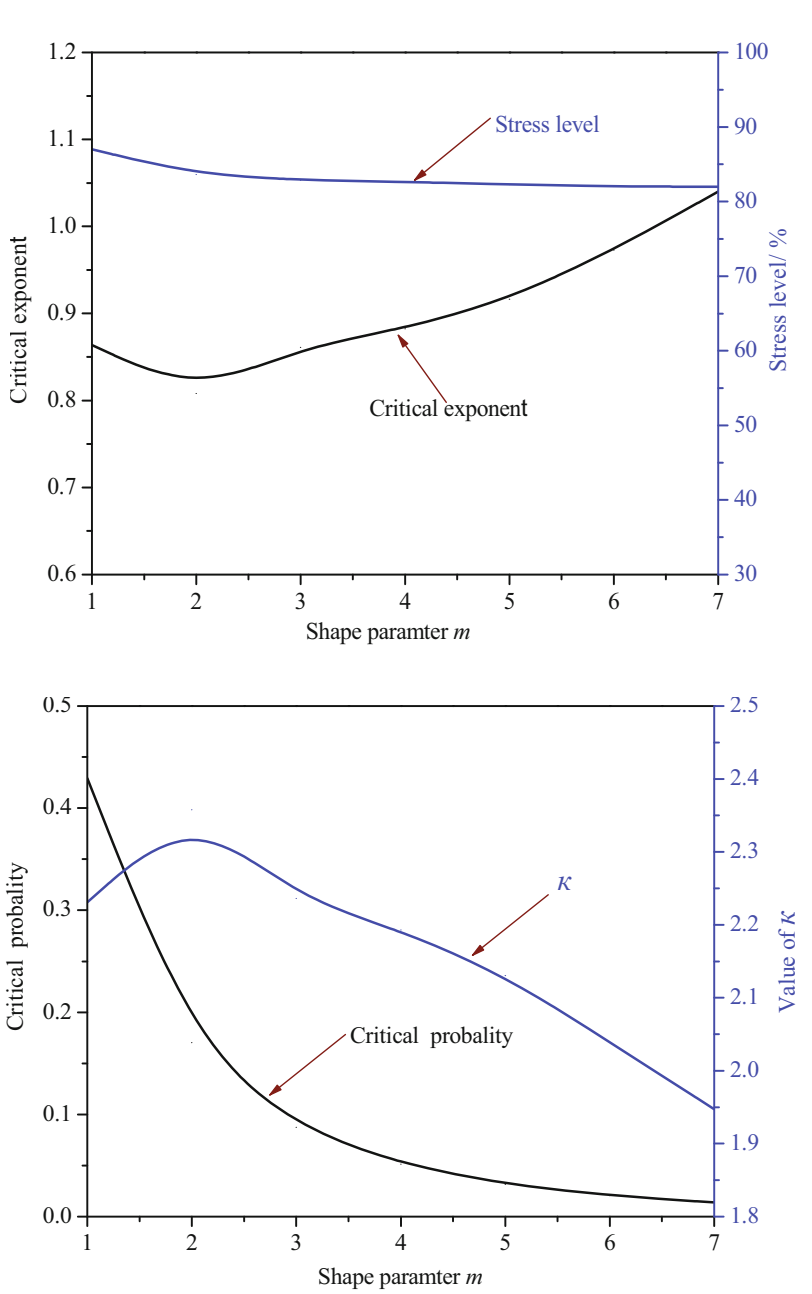

Fig. 4. The variation of critical probality, critical exponent, and critical stress level with the shape: (a) critical exponent and critical stress level, and (b) value of κ and critical probality.

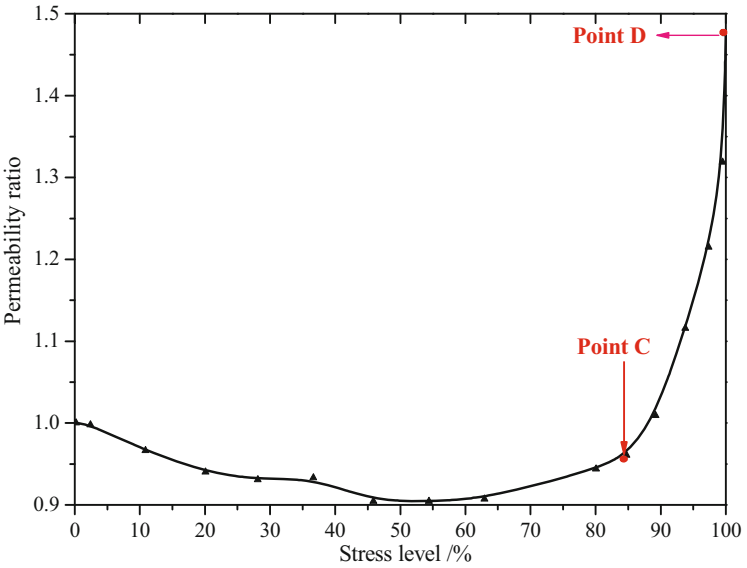

Fig. 5. Relationships of stress level *versus* permeability of Darley sandstone.

Correlation length is an important physical quantity for the renormalization group theory, which is used to mark the characteristics of permeability group. Near the threshold, the correlation length ξ can be expressed as

$$\xi = \xi_0 \left| p_c - p_1^{(n)} \right|^{-\nu} , \tag{16}$$

where ν is the index of correlation length, and ξ_0 is the proportional constant corresponding to unit interval size.

Considering the scale invariance of the renormalization group theory, we have

$$\xi = \xi_0' \left| p_c - p_1^{(n+1)} \right|^{-\nu} , \tag{17}$$

where $\xi_0' / \xi_0 = b$; b is the scale factor, which is obtained by $b = N^{d-1}$; N is the block number of initial level in the renormalization transformation; and d is the spatial dimension.

According to Fig. 3, the value of b is 2. Combining Eqs. 16 with 17, one has

$$\nu = \frac{\ln b}{\ln\left(p_c - p_1^{(n)} \Big/ p_c - p_1^{(n+1)} \right)} . \tag{18}$$

When the broken probability p is near to the critical value, there is

$$\frac{p_c - p_1^{(n)}}{p_c - p_1^{(n+1)}} \to \left.\frac{dp_{n+1}}{dp_n}\right|_{p^*} . \tag{19}$$

Let $\kappa = dp_{n+1}/dp_n$. When $\kappa > 0$, it means the unstable fixed point (critical point). Then we have:

$$v = \ln b / \ln \kappa . \tag{20}$$

The critical exponents of two-dimension renormalization group are shown by Fig. 4.

When the broken probability is lower than the percolation threshold p_c, the broken cells are almost isolated from each other, with less interaction. Contrarily, when the rupture probability is close to the percolation threshold p_c, the correlation length of broken cells increases suddenly, which results in the random, disordered broken cells cluster?

The renormalization group probability of destruction is then employed to calculate the stress at the threshold point of destruction, or the critical point, the stress corresponding to the peak strength, and then the critical stress level. As the permeability increases drastically near to the critical point C, the observation of the evolution of permeability may provide a new approach to identifying the critical point C in the stress-strain curve.

4. CASE STUDIES AND DISCUSSION

Case 1: Triaxial compression test of different sedimentary rock samples

Rock samples (shown in Table 1) were obtained from Yanzhou, Shandong, and cut into cylinders 50 mm in diameter and 100 mm long. They were tested on an electro-hydraulic servo-controlled testing machine (MTS815).

The test result is shown in Figs. 2 and 6. Based on the level of permeability (stress) change *versus* strain level (the stress level is normalized relative to its peak value, and the permeability ratio refers to the value of permeability normalized by the initial permeability obtained from experiments on rock samples), the variation of permeability with stress-strain level can be separated into 3 phases:

(i) In the compaction and elastic phases, permeability decreases with a very small degree with increasing stress (strain), which is mainly due to the closing of original micro fissures and pores.

(ii) After the elastic limited stress is reached, with the increase of loading, micro cracks appear and gradually expand. In this process, the permeability remains unchanged or slightly increases.

(iii) Near to the Point C, plenty of micro cracks initiate and grow rapidly, and micro breaking is developed spatially in rows along the potential break-

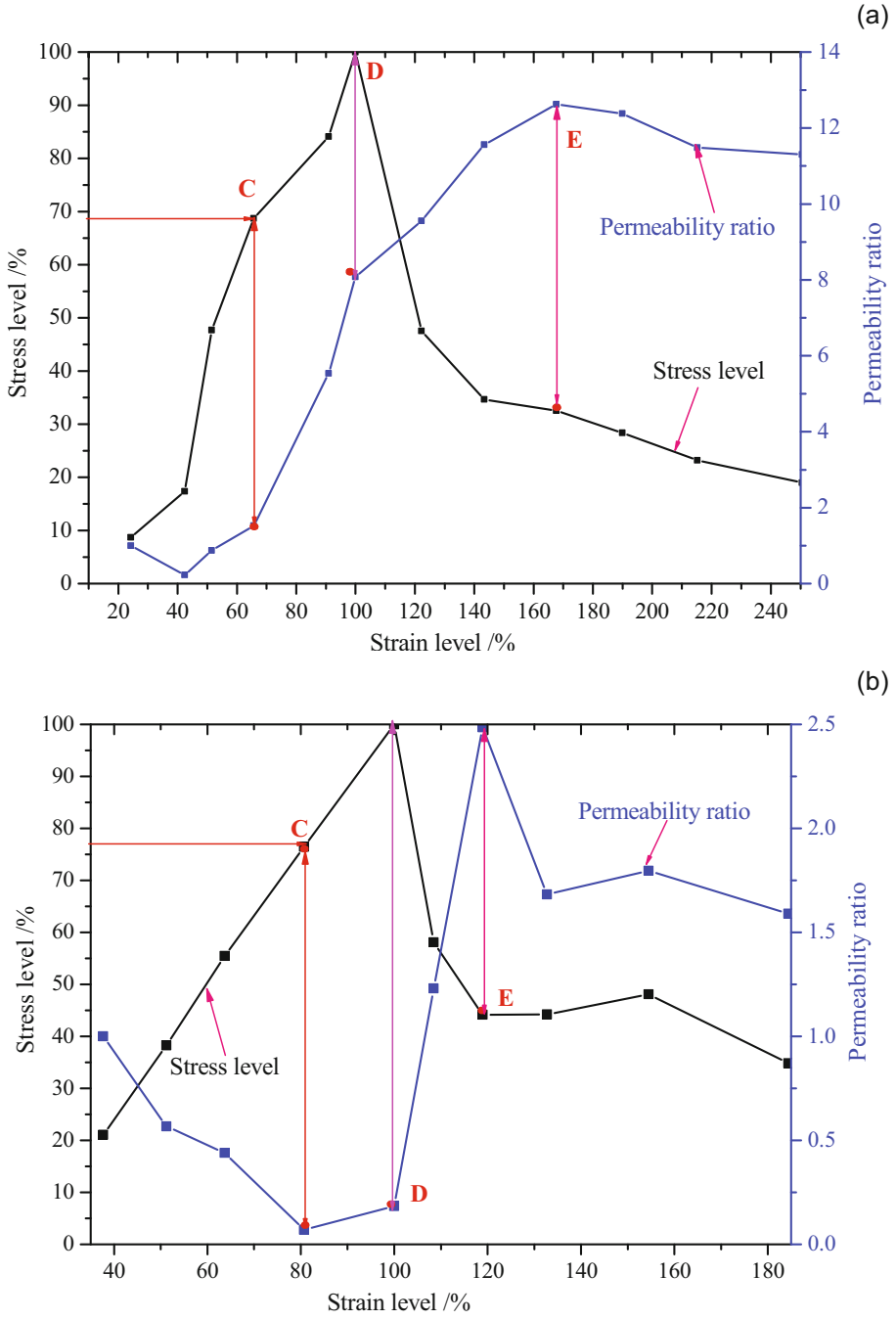

Fig. 6. Continued on next page.

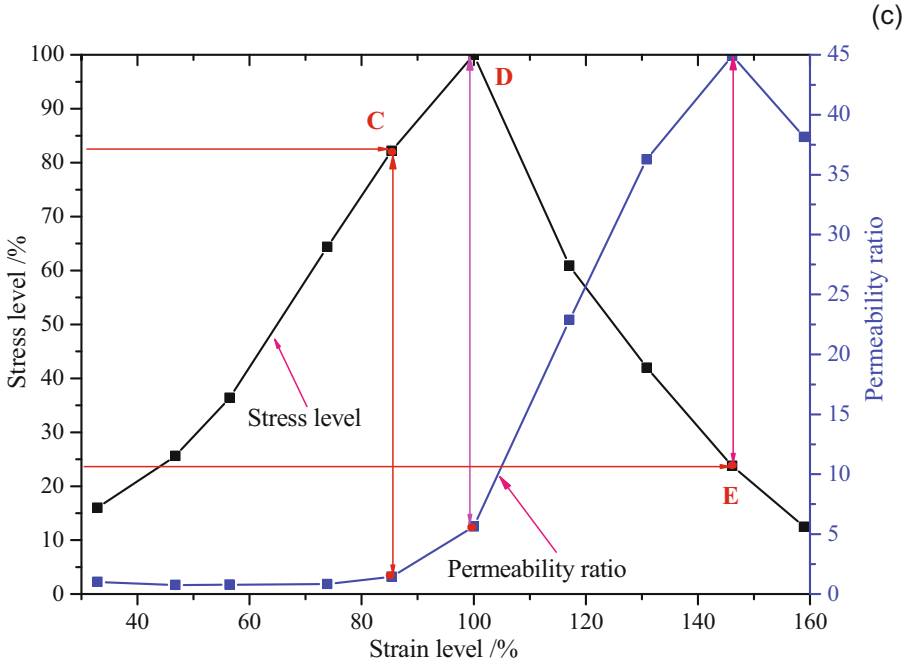

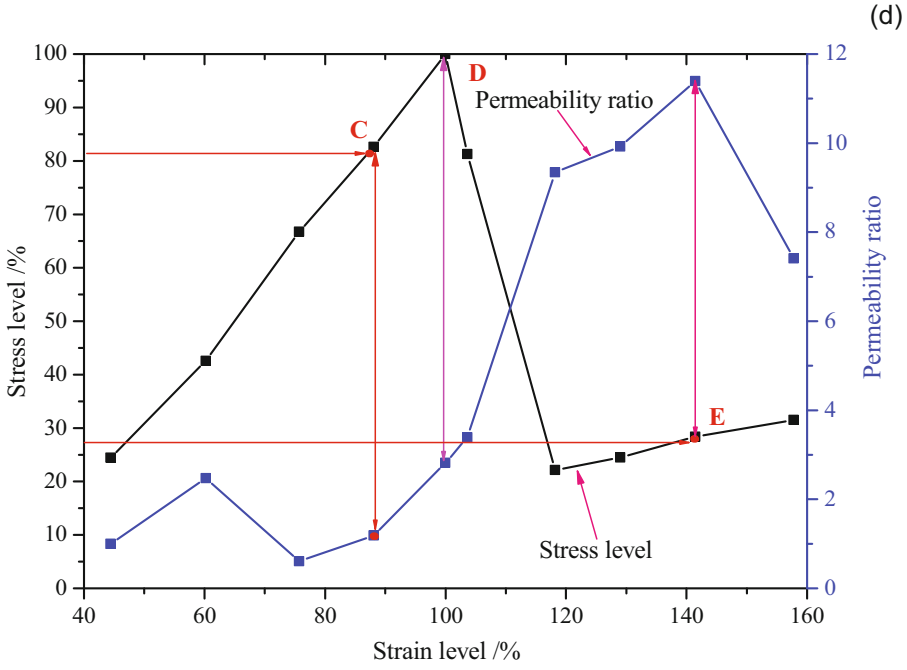

Fig. 6. Continued on next page.

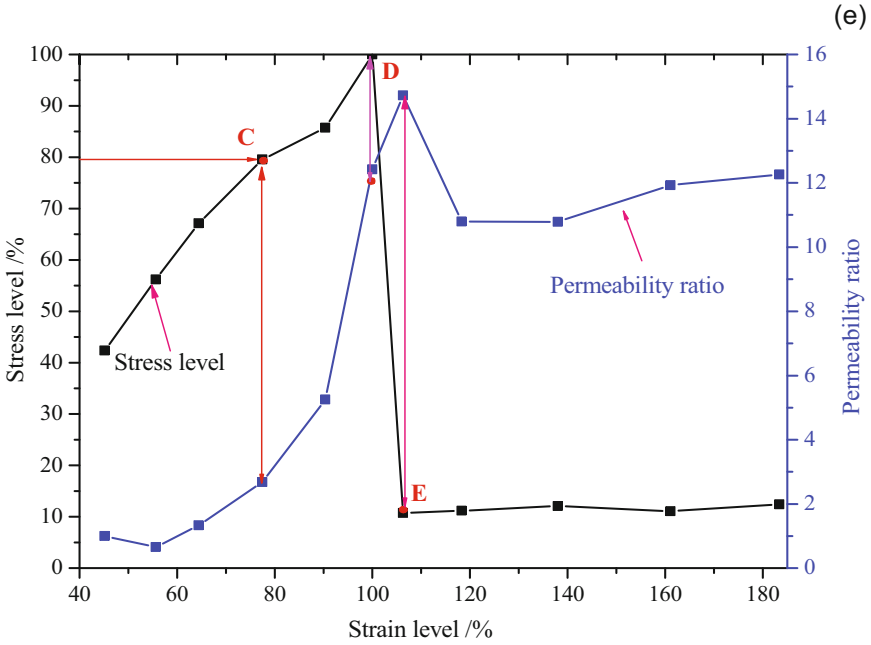

Fig. 6. Relationship between permability, stress level and strain level: (a) limestone (sample 6), (b) medium sandstone (sample 9), (c) medium sandstone (sample 10), (d) fine sandstone (sample 11), and (e) fine sandstone (sample 13).

ing planes until the micro cracks eventually become connected with each other (Fig. 3), as indicated by the location of strain, and accelerated increase of volumetric strain at the cracks. In this phase, permeability has a precipitous increase.

From Fig. 6 and Table 1, we can infer that the stress level at the threshold point of destruction C is approximately 80% of the experimental result. This also suggests that the variation of rock permeability can reflect the changes of stress state, which may provide very useful information on rock stability.

Case 2: Triaxial compression test of granite sample

Rock samples were obtained from the Jining, Shandong, and cut into $\Phi\ 50 \times 100$ mm cylinders. They were tested on an electro-hydraulic servo-controlled testing machine (MTS815).

In the compaction and elastic phases, the permeability declines slightly with the increase of stress, mainly resulting from the closing of original micro fissures and pores (Fig. 7). When the ratio between the loading stress and peak stress near the point C (the average stress level is about 80%), the permeability increases sharply, with a jump in the vicinity of the yield point.

(a)

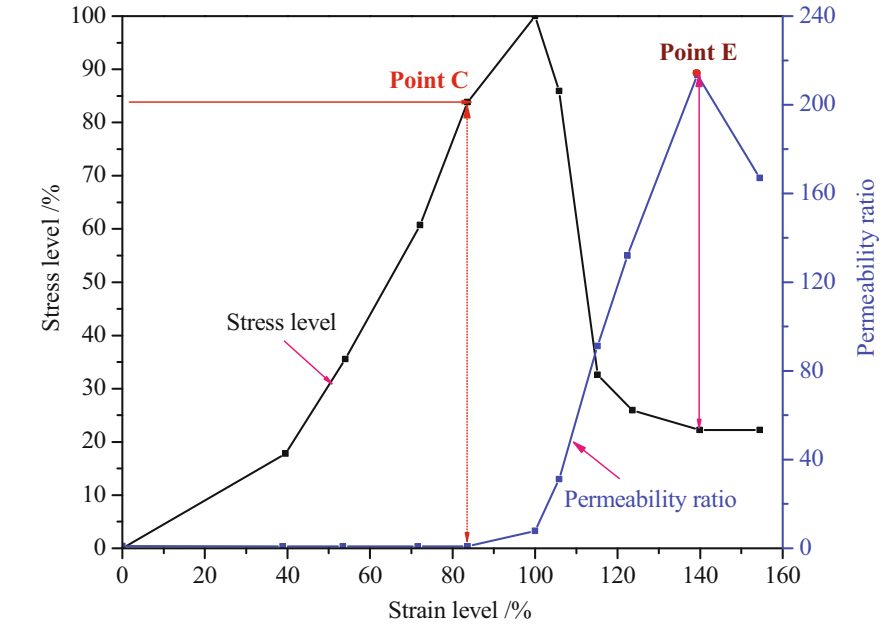

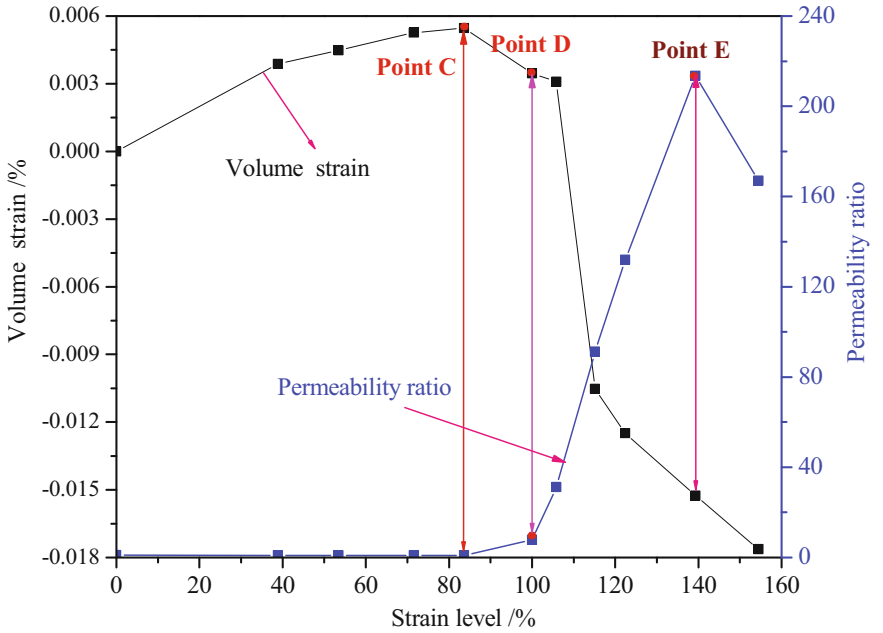

Fig. 7. Continued on next page.

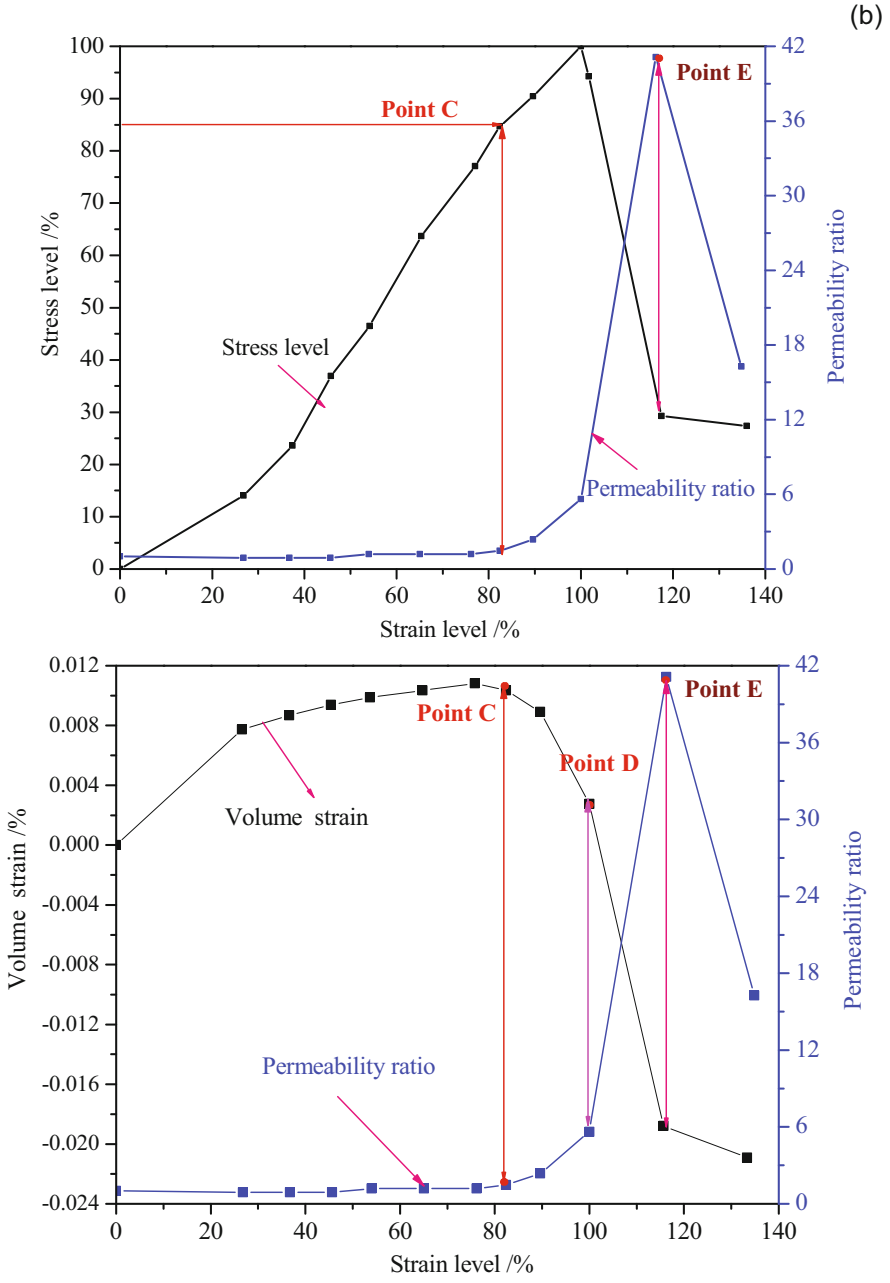

Fig. 7. Relationship between permability, stress level, and strain level of granite samples: (a) sample 1 (confining pressure 4.0 MPa, pore pressure 2.8 MPa), and (b) sample 2 (confining pressure 6.0 MPa, pore pressure 2.8 MPa).

5. CONCLUSIONS

Generalized crack damage threshold is studied in this paper by monitoring stress, strain, and the evolution of permeability during loading processes and theoretically analyzing the stress and strain at the critical point, and the following conclusions are obtained:

- The evolution of permeability varies with the stages of rock fracturing during the process of compression. In the vicinity of the threshold point C (crack coalescence), with the rapid generation and growth of micro cracks inside the rocks, the permeability would increase in a large amount.
- In agreement with the statistical mean of the data collected from laboratory tests, onset of fracture coalescence starts at stress levels of approximately 80% of the peak strength, as predicted with the renormalization group probability of destruction.
- In most cases, the permeability increases sharply at the critical point in rock stress-strain curve. Observing the evolution of permeability may provide a new approach to identifying the critical point (yield point) C in the stress-strain curve.

These conclusions need more experiments for validation, and further investigation on their robustness under various conditions, so that physical predicative methods can be developed for recognizing the threshold information of destruction, promoting the interaction and incorporation of experimental science, rock mechanics, geophysics, and other subjects.

Acknowledgments. This research was supported by the State Basic Research and Development Program of China (No. 2013CB036003), the Project Funded by the Priority Academic Program Development of Jiangsu Higher Education Institutions, the Project supported by the National Science Youth Foundation of China (Grants Nos. 41102201, 41302233, 51309222) and the Project funded by China Postdoctoral Science Foundation (No. 2012M520376).

References

Allègre, C.J., J.L. Le-Mouel, and A. Provost (1982), Scaling rules in rock fracture and possible implications for earthquake prediction, *Nature* **297**, 5861, 47-49, DOI: 10.1038/297047a0.

Anifrani, J.-C., C. Le Floch, D. Sornette, and B. Souillard (1995), Universal log-periodic correction to renormalization group scaling for rupture stress pre-

diction from acoustic emissions, *J. Phys. I France* **5**, 6, 631-638, DOI: 10.1051/jp1:1995156.

Brace, W.F., J.B. Walsh, and W.T. Frangos (1968), Permeability of granite under high pressure, *J. Geophys. Res.* **73**, 6, 2225-2236, DOI: 10.1029/JB073i006p02225.

David, C., B. Menendez, W. Zhu, and T.F. Wong (2001), Mechanical compaction, microstructures and permeability evolution in sandstones, *Phys. Chem. Earth A*, **26**, 1-2, 45-51, DOI: 10.1016/S1464-1895(01)00021-7.

Jiang, Z., L. Ji, R. Zuo, and L. Cao (2002), Correlativity among rock permeability and strain, stress under servo-control condition, *Chin. J. Rock Mech. Eng.* **21**, 10, 1142-1446 (in Chinese).

Liu, H.L., T.H. Yang, Q.L. Yu, and S.-K. Chen (2009), Experimental study on fluid permeation evolution in whole failure process of tuff, *J. Northeast. Univ. (Nat. Sci.)* **30**, 7, 1030-1033 (in Chinese).

Lock, P.A., X. Jing, and R.W. Zimmerman (2002) Predicting the permeability of sandstone from image analysis of pore structure, *J. Appl. Phys*. **92**, 10, 6311-6319, DOI: 10.1063/1.1516271.

Lockner, D.A., J.D. Byerlee, V. Kuksenko, A. Ponomarev, and A. Sidorin (1992), Observations of quasistatic fault growth from acoustic emissions. **In:** B. Evans, and T.F. Wong (eds.), *Fault Mechanics and Transport Properties of Rocks*, International Geophysics, Vol. 51, Academic Press, New York, 3-31, DOI: 10.1016/S0074-6142(08)62813-2.

Martin, C.D. (1993), The strength of massive Lac du Bonnet granite around underground openings, Ph.D. Thesis, University of Manitoba, Manitoba, Canada.

Martin, C.D. (1997) Seventeenth Canadian Geotechnical Colloquium: The effect of cohesion loss and stress path on brittle rock strength, *Can. Geotech. J.* **34**, 5, 698-725, DOI: 10.1139/t97-030.

Mordecai, M., and L.H. Morris (1971), Investigation into the changes of permeability occurring in a sandstone when failed under triaxial stress conditions. **In:** G.B. Clark (ed.), *Dynamic Rock Mechanics (Proc. 12th Ann. Rock Mech. Symp., 16 November 1970, Rolla, USA)*, AIME, New York, 221-239.

Paterson, M.S. (1978), *Experimental Rock Deformation – The Brittle Field*, Minerals and Rocks, Springer, Berlin Heidelberg.

Paterson, M.S., and T.F. Wong (2005), *Experimental Rock Deformation – The Brittle Field*, 2nd ed., Springer, Berlin Heidelberg, 347 pp.

Qin, S.Q., Y.Y. Wang, and P. Ma (2010a), Exponential laws of critical displacement evolution for landslides and avalanches, *Chin. J. Rock Mech. Eng*. **29**, 5, 873-880, DOI: 1000-6915(2010)05-0873-08 (in Chinese).

Qin, S.Q., X.W. Xu, P. Hu, Y.Y. Wang, X. Huang, and X.H. Pan (2010b), Brittle failure mechanism of multiple locked patches in a seismogenic fault and exploration of a new approach to earthquake prediction, *Chin. J. Geophys.* **53**, 4, 1001-1014, DOI: 10.3969/j.issn.0001-5733.2010.04.02 (in Chinese).

Smalley, R.F., D.L. Turcotte, and S.A. Solla (1985), A renormalization group approach to the stick-slip behavior of faults, *J. Geophys. Res.* **90**, B2, 1894-1900, DOI: 10.1029/JB090iB02p01894.

Sornette, D. (2000), Critical Phenomena in Natural Sciences. Chaos, Fractals, Selforganization and Disorder: Concepts and Tools, Springer series in synergetics, Springer, Berlin Heidelberg.

Sornette, D., and J.V. Andersen (1998), Scaling with respect to disorder in time-to-failure, *Eur. Phys. J. B* **1**, 3, 353-357, DOI: 10.1007/s100510050194.

Sulem, J., and H. Ouffroukh (2006), Shear banding in drained and undrained triaxial tests on a saturated sandstone: Porosity and permeability evolution, *Int. J. Rock Mech. Min. Sci.* **43**, 2, 292-310, DOI: 10.1016/j.ijrmms.2005.07.001.

Sun, Q., Z.Q. Jiang, and S.Y. Zhu (2012), Experimental study on permeability of soft rock of Beizao Coal Mine, *Chin. J. Geotech. Eng.* **34**, 3, 540-545, DOI: 1000-4548(2012)03-0540-06 (in Chinese).

Tang, C.A., H. Liu, P.K.K. Lee, Y. Tsui, and L.G. Tham (2000), Numerical studies of the influence of microstructure on rock failure in uniaxial compression – Part I: effect of heterogeneity, *Int. J. Rock Mech. Min. Sci.* **37**, 4, 555-569, DOI: 10.1016/S1365-1609(99)00121-5.

Walsh, J.B., and W.F. Brace (1984), The effect of pressure on porosity and the transport properties of rock, *J. Geophys. Res.* **89**, B11, 9425-9431, DOI: 10.1029/JB089iB11p09425.

Wang, H.L., W.Y. Xu, and S.Q. Yang (2006), Experimental investigation on permeability evolution law during course of deformation and failure of rock specimen, *Rock Soil Mech.* **27**, 10, 1703-1708 (in Chinese).

Wong, T.F., C. David, and W. Zhu (1997), The transition from brittle faulting to cataclastic flow in porous sandstones: Mechanical deformation, *J. Geophys. Res.* **102**, B2, 3009-3025, DOI: 10.1029/96JB03281.

Wong, T.F., R.H.C. Wong, K.T. Chau, and C.A. Tang (2006), Microcrack statistics, Weibull distribution and micromechanical modeling of compressive failure in rock, *Mech. Mater.* **38**, 7, 664-681, DOI: 10.1016/j.mechmat.2005.12.002.

Xue, L. (2014), A potential stress indicator for failure prediction of laboratory-scale rock samples, *Arab. J. Geosci.*, DOI: 10.1007/s12517-014-1456-1.

Yang, Y.J., J. Chu, D.Z. Huan, and L. Li (2008), Experimental of coal's strain-permability rate under solid and liquid coupling condition, *J. China Coal Soc.* **33**, **7**, 760-764, DOI: 10.3321/j.issn:0253-9993.2008.07.008 (in Chinese).

Zhang, R., Z.Q. Jiang, Q. Sun, and S.Y. Zhu (2013), The relationship between the deformation mechanism and permeability on brittle rock, *Nat. Hazards* **66**, 2, 1179-1187, DOI: 10.1007/s11069-012-0543-4.

Zhu, W., and T.F. Wong (1996), Permeability reduction in a dilating rock: Network modeling of damage and tortuosity, *Geophys. Res. Lett.* **23**, 22, 3099-3102, DOI: 10.1029/96GL03078.

Zhu, W., and T.F. Wong (1997), The transition from brittle faulting to cataclastic flow: Permeability evolution, *J. Geophys. Res.* **102**, B2, 3027-3041, DOI: 10.1029/96JB03282.

Zhu, W., and T.F. Wong (1999), Network modeling of the evolution of permeability and dilatancy in compact rock, *J. Geophys. Res.* **104**, B2, 2963-2971, DOI: 10.1029/1998JB900062.

Zoback, M.D., and J.D. Byerlee (1975a), Permeability and effective stress, *Bull. Am. Assoc. Petrol. Geol.* **59**, 154-158.

Zoback, M.D., and J.D. Byerlee (1975b), The effect of microcrack dilatancy on the permeability of westerly granite, *J. Geophys. Res.* **80**, 5, 752-755, DOI: 10.1029/JB080i005p00752.

Received 9 December 2013
Received in revised from 18 May 2014
Accepted 9 July 2014